ELSEVIER

Earth and Planetary Science Letters 139 (1996) 509–519

EPSL

Rock-magnetic signature of gas hydrates in accretionary prism sediments

Bernard A. Housen [a,*], Robert J. Musgrave [b]

[a] *Institute for Rock Magnetism, University of Minnesota, 293 Shepherd Laboratories, 100 Union Street SE, Minneapolis, MN 55455-0128, USA*

[b] *School of Earth Sciences, La Trobe University, Bundoora, VIC 3083, Australia*

Received 21 November 1995; accepted 25 November 1995

Abstract

Sediments from two Ocean Drilling Program Leg 146 sites from the Cascadia margin of western North America have magnetic properties indicating diagenesis of magnetic minerals associated with the presence of gas hydrates. Two indices combining coercivity, remanence, and susceptibility parameters, D_{JH} ($=\{J_{rs}/J_s\}/\{H_{cr}/H_c\}$) and D_S ($=\{J_{rs}/k\}/H_{cr}$), when combined with thermo-magnetic data, can be diagnostic of these changes. At Site 892, D_S values are distinctly higher and more scattered above the bottom simulating seismic reflector (BSR), which marks the base of the hydrate stability zone. Within the hydrate stability zone at Site 892, D_{JH} shows two trends: an increase from about 50 mbsf to the BSR at 73 mbsf, corresponding to an expected increase in hydrate concentration near the BSR; and a second increase upwards from 50 mbsf to peak values at less than 21 mbsf, associated with hydrate recovered in cores above 19 mbsf. At Site 889/890 D_{JH} increases downhole to about 285 mbsf, substantially below the BSR at 225 mbsf. High D_{JH} sediments within a low Cl^- zone at this site have magnetic mineralogies which are dominated by fine-grained magnetic sulfides, whereas sediments from above and below this zone are characterised by magnetite–magnetic sulfide mixes. This trend at Site 889/890 is consistent with an interpretation based on pore-water geochemistry (low Cl^-) and bottom-water temperature that a 'fossil gas hydrate zone' extended downwards to about 295 mbsf during the last glacial.

The observed changes in magnetic properties can be attributed to steps in the reduction series from magnetite through SD greigite to pyrite (or to overgrowth of SD greigite to MD size). Diagenetic growth of magnetic iron sulfides (greigite and/or pyrrhotite) has been reported in other accretionary wedge sediments. Thermal demagnetization of multi-component isothermal remanent magnetization (mIRM) indicates the presence of a low-coercivity magnetic mineral with an unblocking temperature (T_{ub}) between 310° and 350°C. High J_{rs}/k ratios suggest that the low-coercivity, low unblocking temperature mineral is predominantly greigite rather than pyrrhotite. A low- to medium-coercivity mineral with T_{ub} ca. 580°C — magnetite — is also present in varying amounts.

Hydrate apparently controls the presence of greigite by incorporating H_2S, shown to be present as a hydrate phase together with methane in hydrate recovered at Site 892. Release of H_2S below the base of the hydrate layer allows overgrowth of greigite grains to MD size or the conversion of some of the greigite to pyrite.

Keywords: ODP Site 892; accretionary wedges; gas hydrates; remanent magnetization; greigite

* Corresponding author. E-mail: house009@gold.tc.umn.edu

SSDI 0012-821X(95)00245-6

1. Introduction

One of the scientific objectives of Ocean Drilling Program Leg 146 was to examine the occurrence of gas hydrates and their relationship to the characteristic bottom simulating seismic reflector (BSR) and style of fluid flow at two sites on the Cascadia accretionary prism [1]. Site 889 (and its nearby companion, Site 890, which sampled only the upper 48 m of sediments), located off Vancouver Island (Fig. 1), represents an area of diffuse fluid flow through the accretionary prism sediments. Site 892, off the Oregon coast, represents an area of focused fluid flow. Samples of gas hydrates were recovered from Site 892 in the interval from 2 to 19 metres below sea floor (mbsf), and were inferred to occur at Site 889/890 from 150 to 225 mbsf, based on low core temperatures and geochemical evidence [2].

Shipboard palaeomagnetic study of samples from Sites 888–892 found an intriguing contrast in magnetic behavior between the two sites which contained gas hydrates (Sites 889/890 and 892) and those which did not (Sites 888 and 891). The latter two sites both exhibited stable remanent magnetizations, allowing a reliable magnetostratigraphy to be constructed [3,4]. The natural remanent magnetization of sediments from the two sites containing gas hydrates (Sites 889/890 and 892) was generally resistant to alternating field demagnetization and did not yield a reliable magnetostratigraphy [2,5]. In order to explore the differences in remanence behavior associated with sediments bearing gas hydrates, detailed rock-magnetic study of samples from Sites 889/890 and 892 was conducted.

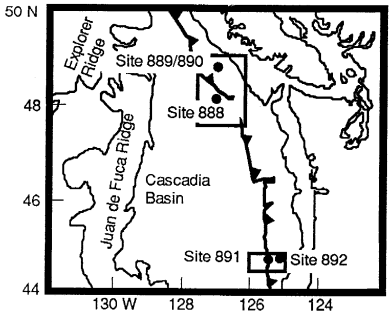

Fig. 1. Location of Ocean Drilling Program Leg 146, Sites 888–892.

Authigenic sulfides were found throughout the sequence at both sites in a number of forms: concentrated in black, fine-grained layers and patches; partially or completely replacing grains of 'glaucony'; within carbonate concretions; and disseminated through the sediment [2,5]. Sulfides take both cube and framboidal habits. X-ray diffraction studies on randomly oriented bulk powder samples indicated the presence of pyrite; a peak at 2.07 Å in two samples from Site 889/890 at about 40 mbsf may indicate the presence of pyrrhotite, although other peaks characteristic of pyrrhotite were masked by other sediment components. Optical examination of smear slides showed the opaque mineralogy to be dominated by sulfides, with sporadic grains of magnetite, ilmenite and manganese minerals. No evidence was seen for the presence of titano-haematites and the strongly reduced state of the sediments cored on Leg 146 [1] argues against the survival of maghemite. Hence, the likely magnetic mineralogy at these sites is restricted to magnetite and magnetic iron sulfides (greigite and/or pyrrhotite). A similar range of magnetic mineralogy was determined by a range of rock magnetic methods from reduced accretionary wedge sediments from the Chile margin [6].

Rock-magnetic studies of marine sediments have focused primarily on the early diagenesis of magnetic sulfides and oxides within the first few meters of the sediment column [7,8]. The progressive diagenetic change from iron oxides, to iron monosulfides (e.g. mackinawite) to (magnetic) iron sulfides (greigite and pyrrhotite) and, finally, to pyrite under reducing conditions is well known [9]. Most occurrences of diagenetic magnetic sulfides in deeper sediments, or in ancient sediments, are thought to have been produced during this shallow level, early diagenesis (e.g., [10]). Recently, production of new magnetic minerals (either iron oxides or iron sulfides) in sediments has been attributed to the migration of hydrocarbons [11], or of methane and fluids [6,12] at depths greater than 500 mbsf. The actual mechanism of magnetic mineral diagenesis in these cases is less well known, but is thought to be the result of reducing conditions associated with methane or other organic materials.

Gas hydrates are clathrates (cage structures) of water and some type of gas (either methane, ethane, propane, hydrogen sulfide or carbon dioxide) [13].

Methane hydrate is thought to be the most common natural form of gas hydrate and occurrences of these hydrates have been reported from many locations on continental margins and beneath regions of permafrost [14]. Bottom simulating reflectors are thought to result from the impedance contrast between hydrate-bearing sediments and sediments with free methane in pore spaces, which develops at the thermally controlled base of the zone of methane hydrate stability [15]. The effects of gas hydrates on the mineralogy of marine sediments are not well studied. Of the few such studies, diagenesis of siderite ($FeCO_3$) in sediments from the Blake Ridge was attributed to the presence of gas hydrates [16], as was the occurrence of carbonate nodules from sediments off Sakhalin Island (Okhotsk Sea) [17].

2. Sampling and methods

Samples from Sites 889/890 and 892 were collected during Leg 146 of the Ocean Drilling Program. Standard 6 cm^3 sediment specimens were cut from the split cores and placed in plastic cubes, which were then sealed to prevent excessive drying of the samples. At least one sample per core was collected (each core usually representing 9.5 m of section), and a total of 114 samples were measured for this study. Magnetic hysteresis measurements were made with the vibrating sample magnetometer (VSM) at the Institute for Rock Magnetism at the University of Minnesota. A peak applied field of 0.5–1.0 T was used for the hysteresis measurements and the results were corrected for the paramagnetic and diamagnetic contributions of the matrix minerals (primarily paramagnetic clays). Values of saturation magnetisation (J_s), saturation remanent magnetisation (J_{rs}) and coercivity (H_c) were directly obtained from the hysteresis measurements, while coercivity of remanence (H_{cr}) was obtained by step-wise application of a back-field isothermal remanence to remove the saturation remanence. Thermal demagnetisation of a multi-component isothermal remanent magnetisation (mIRM) [18] was used to identify further the magnetic minerals in these sediments. Orthogonal applied fields of 1.4 T, 0.4 T, and 0.05 T were applied using an electromagnet housed at the University of Michigan Paleomagnetic Laboratory. The mIRM was then thermally demagnetised with an ASC thermal demagnetiser, using 18–20 thermal steps from 80°C to 600°C. After each thermal treatment, the remanence was measured using a 2-G 3-axis cryogenic magnetometer. Both the thermal demagnetiser and cryogenic magnetometer are housed in a low-field room in the University of Michigan Palaeomagnetic Laboratory. Magnetic susceptibility measurements (k) were made with a KLY-2 Kappabridge, also housed in the University of Michigan Palaeomagnetic Laboratory.

3. Results

3.1. Thermal demagnetisation of mIRM

Thermal demagnetisation of mIRM indicated that two magnetic phases are present in nearly all samples from both sites. In all cases, the dominant remanence component is the 0.05 T component,

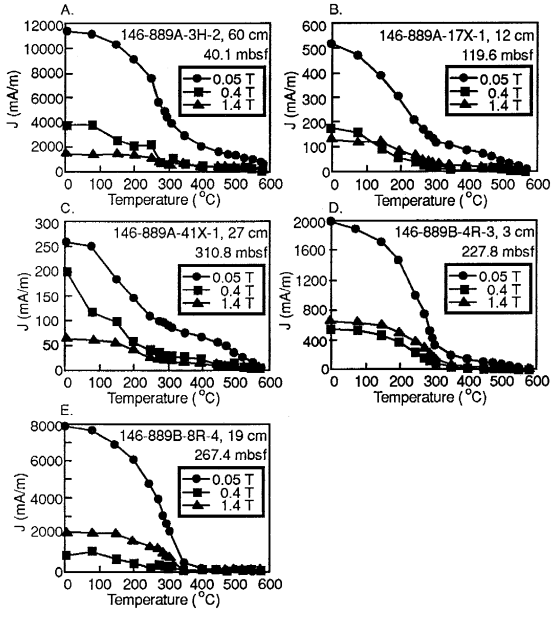

Fig. 2. Multi-component IRM (mIRM) thermal demagnetization results from Site 889/890 samples. Magnetization of each component is given in mA/m for each demagnetization step. (A) and (B) Samples from above the low-chloride zone, which have low D_{JH} values. (C) Sample from within the low-chloride zone, below the interval with high D_{JH}. (D) and (E) Samples from the high D_{JH} interval within the zone of low pore-water Cl^-.

which will be carried by grains with relatively low coercivities: magnetite, greigite, or very large (>40 μm) pyrrhotite. This component has two unblocking temperatures (T_{ub}), one between 290° and 310°C (corresponding to greigite or pyrrhotite (because maghemite can be ruled out by the reducing pore-water chemistry), which decompose on heating in air between about 300° and 400°C [6,10,19]), the other at 560° to 580°C (corresponding to the Curie point of magnetite). Results of the mIRM analysis at Site 889/890 show a clear difference in magnetic mineralogy between the samples from within the low-chloride zone and those from sediments above and below this zone (Fig. 2). The samples between the top of the low-chloride zone and 285 mbsf have a remanence that is carried almost entirely by the low T_{ub} phase (probably greigite), with $>75\%$ of the total mIRM removed after 350°C (Fig. 2D and E). These samples also have a higher fraction of the remanence carried by the 1.4 T mIRM component relative to the 0.4 T component. The 1.4 T component will only be carried by fine-grained magnetic sulfides, rather than magnetite. Samples from above and below this interval have mIRM results which indicate a larger proportion of magnetite, because 40–50% of the initial remanence remains after 350°C (Fig. 2A–C). In these samples, the 0.4 T mIRM component is larger than the 1.4 T component, which is also indicative of a lower proportion of magnetic sulfides.

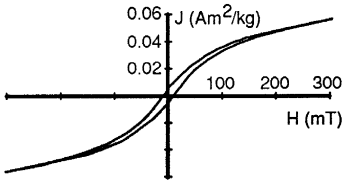

Fig. 3. Hysteresis curve of a typical sediment sample (Sample 146-889A-22X-5, 8–10 cm) from Site 889/890.

3.2. Hysteresis: Site 889 / 890

Hysteresis of all samples from both Sites 889/890 and 892 follows a simple pattern (Fig. 3), without any evidence for 'wasp-waisted' or other unconventional hysteresis cycle patterns. Saturation magnetisation and remanence, susceptibility and hysteresis parameters for the samples from Site 889/890 are plotted against sub-bottom depth in Fig. 4. The

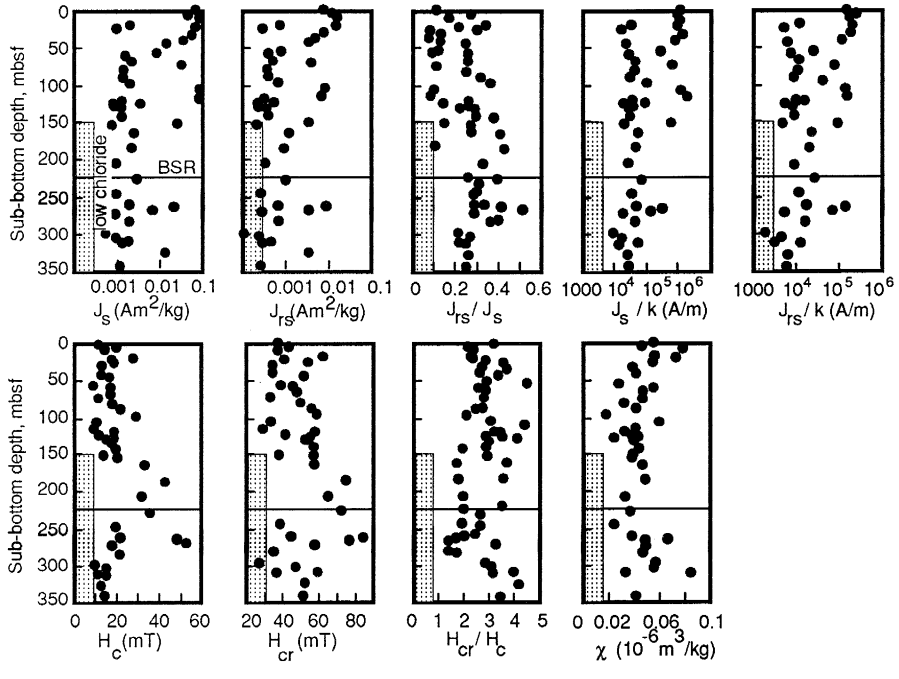

Fig. 4. Plots of remanence, coercivity and susceptibility parameters against sub-bottom depth, Site 889/890.

various hysteresis parameters are functions of the concentration (J_{rs}, J_s and k), average domain state (and hence grain size) (J_{rs}, J_s, k, H_c and H_{cr}), and species (H_c, H_{cr} and k) of the ferrimagnetic minerals in these sediments. Below a sub-bottom depth of about 150 mbsf, corresponding to the top of an interval of low pore-water chloride concentrations [2], both J_s and J_{rs} are less scattered and have lower average values than above 150 mbsf. An interval of elevated H_c and H_{cr} values is also present within the low-chloride zone, but is restricted to between about 185 and 267 mbsf. A small spike, defined by two samples in both J_s and J_{rs} at about 265 mbsf, corresponds to the position of the peak values of H_c and H_{cr}.

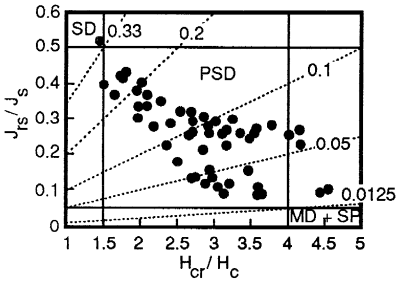

Fig. 5. Plot of J_{rs}/J_s versus H_{cr}/H_c for Site 889/890, divided into fields indicating domain state for any non-interacting magnetic minerals: SD = single-domain; PSD = pseudo-single-domain; MD + SP = multidomain and/or superparamagnetic. Dashed lines indicate contours of the parameter D_{JH}.

Combining the magnetisation and coercivity ratios defines a set of apparent domain state (proportional to grain size) fields valid for any random assemblage of non-interacting magnetic grains [20]. Samples from Site 889/890 are distributed more-or-less linearly within the pseudo-single-domain (PSD) field, extending towards the SD field in one direction, and the joint MD and SPM fields in the other (Fig. 5). The spread of the hysteresis ratios along this trend probably reflects a mixture of magnetic minerals which are fine-grained (SD) and coarse-grained (PSD and MD). Examination of the H_{cr}/H_c and J_{rs}/J_s data with depth (Fig. 4) shows that the samples from the low-chloride zone, which have a magnetic sulfide-dominated mineralogy, are characterised by an overall fine grain size, with results in the SD and the finer portion of the PSD field of Fig. 5. Combined, the mIRM data and the hysteresis data indicate that

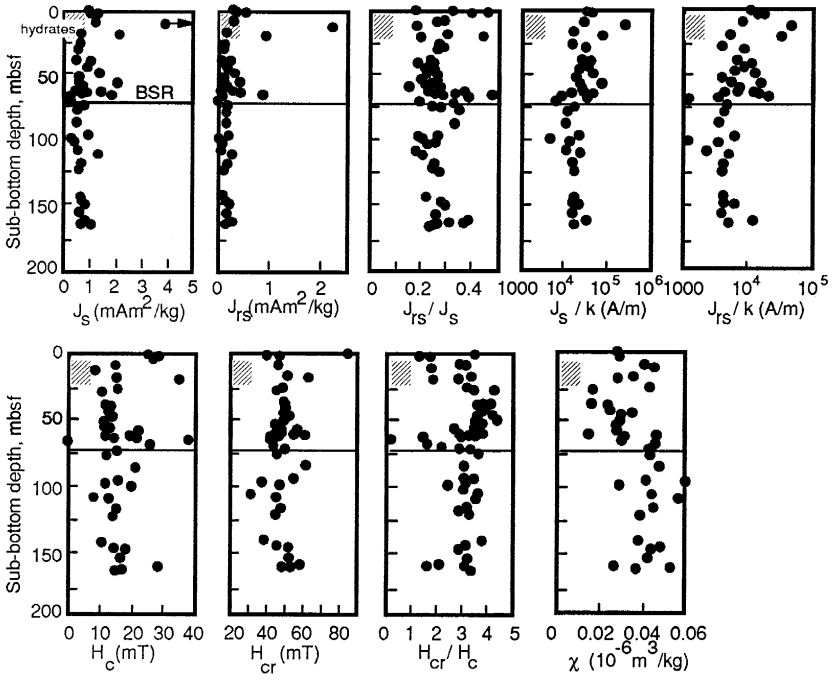

Fig. 6. Plots of remanence, coercivity and susceptibility parameters against sub-bottom depth, Site 892.

the sediments above and below the low-chloride zone at Site 889/890 contain a mixture of magnetite and magnetic sulfides, with both coarse and fine grain sizes. This mineralogy is altered within the low-chloride zone, because nearly all the magnetite is replaced by fine-grained magnetic sulfides.

The ratio J_{rs}/k can be used to distinguish between assemblages of the two likely magnetic sulfides (greigite and pyrrhotite). Pyrrhotite has relatively low values of saturation remanence and high values of susceptibility, and is thus characterised by low J_{rs}/k values [21]. Greigite in lacustrine and marine sediments has been found to have high values of J_{rs} relative to susceptibility, so high J_{rs}/k values can be diagnostic of this mineral in such sediments [10,22–27]. The physical basis for high J_{rs}/k values in natural greigite appears to be due to a relatively large grain size for the single-domain to multi-domain threshold in this mineral [22,25]. For example, samples from marine mudstones and siltstones of the Seabee and Ninuluk Group of Alaska, in which remanence is dominated by greigite, have J_{rs}/k values > 10 kA/m; the majority of these samples have J_{rs}/k between 50 and 175 kA/m [23]. Sediments from these formations with mixtures of greigite (which has replaced magnetite) and surviving iron–titanium oxides have J_{rs}/k values ranging from 2.5 to 30 kA/m. Most samples from Site 889/890 have a J_{rs}/k ratio > 5 kA/m, and all but one sample (at 299 mbsf) have values > 2.5 kA/m, which are consistent with magnetite/greigite mixtures. Although the J_{rs}/k ratio is strongly dependent on grain size, which places limits on its usefulness as a discriminant of mineralogy, comparison of the Leg 146 with Alaskan results suggests that greigite is the most likely carrier of the low T_{ub} mIRM components through most of the cored sequence.

3.3. Hysteresis: Site 892

In contrast to Site 889/890, magnetisation and coercivity behavior at Site 892 show a clear response at or close to the BSR, which was fixed at 73 mbsf by a vertical seismic profile [5] (Fig. 6). Overall, both J_s and J_{rs} have lower values and vary far less than at Site 889/890, and both parameters become scattered towards higher values downhole at Site 892, from about 40 mbsf to about 67 mbsf. Below the BSR J_{rs} and J_s are less scattered, with lower values overall. Two samples between 67 mbsf and the BSR at 73 mbsf have notably lower J_s and J_{rs} values. There is a general increase in J_{rs}/J_s from about 40 mbsf downwards, and a sharp break to higher, scattered values of J_{rs}/J_s at about 63 mbsf. This ratio declines again below the BSR, and appears to return to background values at about 100 mbsf. Elevated J_{rs}, J_s and J_{rs}/J_s values are also scattered in the uppermost 21 mbsf at Site 892, corresponding to the interval (2–19 mbsf) in which gas hydrate samples were recovered from the sediments [5]. There is a further short interval of scattered higher J_{rs}/J_s values at about 162–164 mbsf, near the base of a fault zone identified in Hole 892A. As at Site 889/890, J_s/k and J_{rs}/k at Site 892 mimic the downhole pattern of J_r and J_s, indicating changes in the proportions of magnetic minerals present. Throughout most of the sequence at Site 892, J_{rs}/k exceeds 5 kA/m, suggesting that greigite contributes a significant proportion of the remanence, and $J_{rs}/k > 10$ kA/m (indicating that greigite dominates the remanence) in some samples from each of the three intervals of elevated J_{rs} described above.

Coercivity also apparently responds to the BSR at Site 892. Coercivity of remanence becomes increasingly scattered downhole, from about 50 mbsf to 67 mbsf, and is strongly scattered within the uppermost 21 mbsf; two samples between 67 mbsf and the BSR have reduced H_{cr} values, and H_{cr} below the BSR is strongly scattered. Similar scatter affects H_c below the BSR, and H_c shows distinctly elevated values between 60 mbsf and the BSR and between 0 and 21 mbsf. The H_{cr}/H_c ratio declines sharply at about 63 mbsf, and increases again at the BSR. Low values of H_{cr}/H_c also occur from 0 to 21 mbsf, and near the fault zone at 162–164 mbsf.

Samples from Site 892 also mainly plot in the PSD field on magnetisation versus coercivity ratio plots (Fig. 7). The ratio of the two axes in this plot (i.e., $\{J_{rs}/J_s\}/\{H_{cr}/H_c\}$) is an index of grain size (which we term D_{JH}), with SD-dominated assemblages > 0.33, and MD- or SPM-dominated assemblages < 0.0125. This index cannot distinguish between MD-dominated assemblages and those which are mixes of SPM grains with MD, PSD or SD grains.

Because SPM grains contribute to susceptibility,

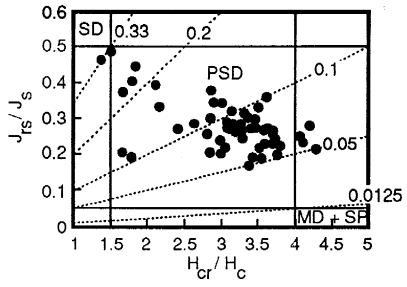

Fig. 7. Plot of J_{rs}/J_s versus H_{cr}/H_c for Site 892; fields and contours as for Fig. 5.

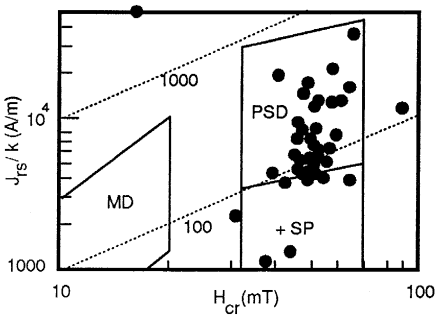

Fig. 8. Plot of J_{rs}/k versus H_{cr} for Site 892, divided into fields indicating domain state for assemblages of non-interacting magnetite grains: PSD = pseudo-single-domain; MD = multidomain; + SP = admixture of superparamagnetic grains. Dased lines indicate contours of the parameter D_S.

but not to remanence, they do not affect H_{cr}, and so samples with a large SPM component have low $(J_{rs}/k)/H_{cr}$ ratios [28], which we term D_S. Empirical measurements of assemblages of magnetite grains define fields for MD, PSD and SPM admixtures on a J_{rs}/k versus H_{cr} plot [29] (Fig. 8); a D_S value of 100 approximately divides the PSD and PSD + SPM fields for magnetite. Changes in D_S, then, may represent either variations in the proportions of magnetic sulfides present, and/or in the proportion of SPM grains. At Site 892, above 67 mbsf (i.e., within the zone of hydrate stability, extending down to within 6 m of the BSR), D_S data (Fig. 9) show a scatter to high values, with a minimum of about 80 $mAm^{-1}T^{-1}$. Highest values of D_S occur in the upper 21 mbsf, in or close to the interval from which hydrates were recovered, and the scatter in D_S trends towards higher maximum values with increasing depth from 30 to 67 mbsf. Below 67 mbsf the D_S data are grouped more closely between about 25 and 100 $mAm^{-1}T^{-1}$, with one higher value near the fault zone at 163 mbsf. Scatter in D_{JH} below 67 mbsf is less, and trends are more clearly defined. High D_{JH} values (> 0.11) at less than 21 mbsf (including scattered values above 0.2) decline with increasing sub-bottom depth, reaching an average of about 0.06 at about 50 mbsf; D_{JH} then sharply increases with increasing depth, reaching average values of around 0.12 at the BSR, with scattered higher values again occurring in the interval from 55 mbsf to the BSR. Below the BSR, the average D_{JH} ratio declines, varying between about 0.07 and 0.1, save for a local peak to around 0.2 near the fault zone.

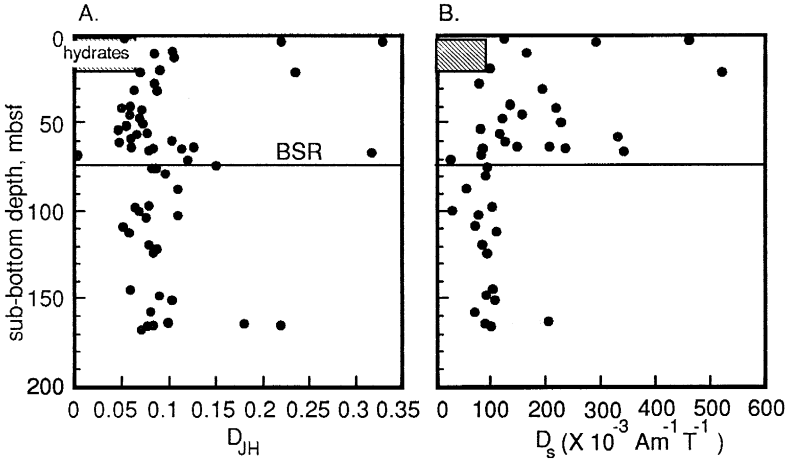

Fig. 9. Sub-bottom depth versus D_{JH} and D_S for Site 892 samples. The interval where hydrates were recovered in cores and the depth of the bottom simulating reflector (BSR) are indicated.

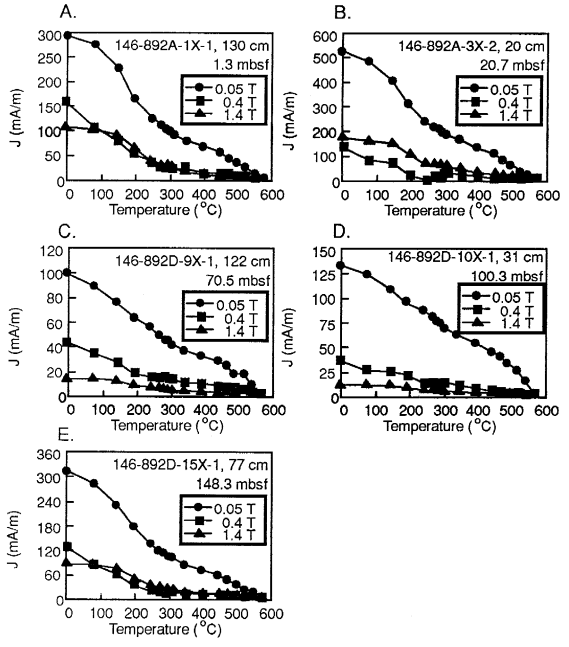

Fig. 10. Multi-component IRM (mIRM) thermal demagnetization results from Site 892 samples. Magnetization of each component is given in mA/m for each demagnetization step. (A) Sample from just above the interval of recovered gas hydrates (2–19 mbsf), with a low D_{JH} value. (B) Sample with a high D_{JH} value, from just below the interval of recovered gas hydrates. (C) Sample with a high D_{JH} value, from just above the BSR (73 mbsf). (D) and (E) Samples below the BSR, with intermediate D_{JH} and low J_{rs}/k values.

The mIRM results from Site 892 do not generally reveal major differences between samples which have higher D_{JH} ratios (Fig. 10B and C) and those which have lower D_{JH} ratios (Fig. 10A). Several samples from below the BSR at Site 892, however, have mIRMs with a single T_{ub} at 570°C, indicating that magnetite is the only magnetic mineral present in significant proportions in these samples (Fig. 10D). The mIRMs from Site 892 also indicate relatively low (< 700 mA/m) saturation remanences.

4. Discussion

Changes in magnetic hysteresis properties are closely associated with the occurrence of gas hydrates at Site 892. Gas hydrates should be stable from the seafloor to the BSR, and are thought to be abundant in two intervals above the BSR at this site. In the upper interval (2–19 mbsf) disseminated to massive gas hydrates were recovered from the sediments. This interval was also marked by low pore-water Cl^-, low core temperatures and very high H_2S contents. These observations were attributed to the dissociation of gas hydrates upon recovery of the sediments [5]. A low Cl^- signal was also found in sediments from 68 mbsf, 5 m above the BSR, and was cited as evidence for the presence of gas hydrates from around 68 mbsf to the depth of the BSR [5]. The two main intervals of high D_{JH} ratios ($>$ 0.11) at Site 892 match almost exactly the intervals in which abundant hydrates were recovered, or were inferred to exist from core chemistry and physical properties. A further short interval of high D_{JH} corresponds to a fault zone at about 162–164 mbsf. High D_S values extend more generally over the whole interval of hydrate stability above the BSR, but reach their peak values in the two intervals of high D_{JH} values. However, the sudden drop in D_S appears to occur about 5 m above the BSR.

No gas hydrates were recovered at Site 889/890, but the presence of hydrates was indicated by a low-temperature measurement from Core 146-889B-3R (215–224 mbsf), by low Cl^- values in pore waters from below 150 mbsf, and by the prominent BSR at 225 mbsf [2]. However, the low Cl^- values persist to depths greater than the BSR at this site. The sediments from the low Cl^- zone contain predominantly fine-grained magnetic sulfides, and can be characterised by relatively high values of D_{JH} (Fig. 11). Below about 285 mbsf at Site 889/890,

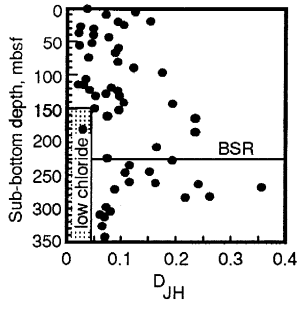

Fig. 11. Sub-bottom depth versus D_{JH} for Site 889/890 samples. The zone of low pore-water Cl^- and the depth of the bottom simulating reflector (BSR) are indicated.

D_{JH} drops to about 0.07–0.08, similar to D_{JH} values measured for samples from Leg 146 sites which contained no hydrate (Sites 888 and 891). Sediments below 285 mbsf also have magnetite-dominated mIRM results (Fig. 2C). An interesting speculation is that the high D_{JH} values in samples from depths below the present-day stability field of methane hydrates reflect changes in the magnetic mineralogy which occurred when hydrate was stable to greater sub-bottom depths (i.e., to about 285 mbsf) during the last glaciation. The base of the gas hydrate stability field was estimated to have been ca. 70 m deeper at Site 889 during the last glaciation [2], so gas hydrates may have been present in the sediments to a depth of ca. 295 mbsf in the recent past. This estimate closely matches the base of the high D_{JH} and sulfide-dominated mIRM zone at Site 889/890, so the rock magnetic data support the hypothesis of a 'fossil gas hydrate zone'.

At Site 892 high values of J_{rs}/k and D_S characterise the zone of gas hydrate stability above the BSR, and a low T_{ub} mineral is present in substantial proportions in samples from above the BSR. Greigite satisfies both the low-T_{ub} and high J_{rs}/k and D_S criteria. Below the BSR lower J_{rs}/k and D_S suggest a decreased proportion of greigite, and several samples from below the BSR indeed indicate that only magnetite is present (e.g., Fig. 10D). Changes in D_{JH}, however, should be dependent only on changes in grain size; intervals of high D_{JH} may be explained by a shift from the PSD-dominant range, in which most of the samples fall, by an increase in the proportion of SD grains and/or a decrease in the proportion of SPM (or MD) grains. As greigite is apparently common in the high D_{JH} zones, the process may involve growth of SD greigite, possibly at the expense of SPM (i.e., very fine grained) magnetite. As sediments accumulate, the base of the hydrate stability field should maintain the same depth below the sediment/water interface (providing bottom-water temperature remains constant), and so the BSR should migrate upwards through the sediment column. Low D_{JH} below the BSR requires that a process operates below the BSR to shift the population of magnetic grains back from SD towards the PSD (or MD) field. The sharp decrease in J_{rs}/k and D_S (which either accompanies the drop in D_{JH}, or possibly occurs a few meters above it) suggests a decrease in the proportion of greigite, and is not consistent with the growth of MD greigite.

What is not known is the link between the production of greigite and the occurrence of gas hydrates. Because greigite is an intermediate product in the reduction of sulfates and organic matter to form pyrite, reduction in the sediments must be arrested somehow in order to preserve the greigite. The process can be halted either due to a lack of reducible organic matter, or lack of iron or sulfur (sulfate or H_2S) needed to complete the process of pyrite formation. At both Sites 889/890 and 892, solid organic matter (in addition to methane) is relatively abundant [2,5], so a lack of organic matter does not appear to be the limiting factor. Site 892 may provide the explanation, as the gas hydrates there incorporated up to 10% H_2S together with the methane [30]. If the H_2S needed to complete the reduction of organic matter to pyrite were locked up in clathrates, intermediate reaction products, such as greigite, may be preserved.

Below the BSR at Site 892, lower values in both D_{JH} and D_S presumably reflect the availability of H_2S (and methane) to push the reduction towards pyrite further towards completion. H_2S at this depth, which lies below the base of the sulfate-reduction zone (about 20 mbsf at Site 892 [5]), could only be supplied by melting hydrate, unless otherwise supplied by active fluid advection from deeper in the accretionary wedge. Some specimens indicate an absence of greigite below the BSR at this site, but at least some greigite may have survived. Changes in the grain size of greigite above and below the base of the 'fossil gas hydrate zone' at Site 889/890 presumably arose during the last glaciation; the SD greigite within the 'fossil zone' may have survived because of the very rapid upward migration of the base of the hydrate layer, which may have allowed H_2S to migrate upwards away from the 'fossil zone' before significant growth of the greigite to MD size or the reduction of greigite to pyrite could occur.

In both the modern hydrate zone at Site 892 and the 'fossil' zone at Site 889/890, the D_{JH} ratio increases downward towards the base of the zone, consistent with the expectation that the proportion of hydrate in pore spaces should increase as the BSR is approached from above [15]. Unexpectedly, over the top 50 m at Site 892 D_{JH} also increases toward the

seafloor. The concentration of methane/H_2S hydrate in the upper 20 m at this site appears to be linked to the presence of a fault intercepted at about 50 mbsf in Hole 892A [5], and the inverted gradient of D_{JH} from 50 to about 20 mbsf may reflect diffusion of methane and H_2S upwards from this fault.

At Site 892 an additional peak in D_{JH} and D_S near the fault zone at about 162–164 mbsf may represent growth of SD greigite in response to a different source of methane and H_2S; as fluids migrating from deeper in the accretionary wedge along faults. Very similar development of SD greigite in response to the fault-controlled migration of methane and H_2S has been inferred from rock-magnetic studies from ODP Site 863, on the Chile margin accretionary wedge [6].

Although conversion of greigite to pyrite, or growth of the greigite to MD size, appear to be limited by the availability of free H_2S, the initial production of greigite in the gas hydrate zone at the top of both sites does not seem to be inhibited by the fact that both methane and H_2S will only be present as hydrates. Other studies [6] have indicated that the production of greigite may be mediated by bacteria in response to the availability of free methane, and microbiological studies have indicated a peak of bacterial activity within the hydrate-bearing sediments at Site 892 [R.J. Parkes, pers. commun., 1994]. It appears that the fixation of methane and H_2S as hydrates does not inhibit the (presumably) bacterial production of greigite; however, further reduction or growth of the greigite is apparently restricted where free H_2S (and methane?) is not available.

The results of this study, together with those of an earlier rock-magnetic study of accretionary wedge sediments cored on ODP Leg 141 [6], serve to confirm that pervasive magnetic mineral diagenesis is not confined to the upper few meters of the sediment column, but can occur at depths of hundreds of meters. What is more, in both cases indirect evidence suggests that this process involves the active mediation by bacteria in the generation of greigite.

Further work is need to explore the magnetic mineralogy and chemistry of these samples in order determine the mechanism of greigite formation, and to explore the link between magnetic mineral diagenesis and the occurrence of gas hydrates.

Acknowledgements

We thank the crew, laboratory personnel, and shipboard scientific party of the JOIDES Resolution during Ocean Drilling Program Leg 146 for their efforts in making collection of these samples as pleasant as possible. Work at the Institute for Rock Magnetism was made possible by the National Science Foundation, the Keck Foundation, and the University of Minnesota. Chris Hunt, Jim Marvin, Bruce Moskowitz, and Subir Banerjee are thanked for their help and comments on the work performed there. We further thank Rob Van der Voo and John Stamatakos for comments and assistance while work was conducted at the University of Michigan. Margaret Hastedt is also thanked for performing some of the hysteresis experiments on behalf of RJM. BAH thanks JOI/USSAC for funds which supported this research. This is IRM contribution 9505. *[MK]*

References

[1] G.K. Westbrook, B. Carson, R.J. Musgrave, et al., Proc. ODP, Init. Rep. 146, part 1, 611 pp., 1994.
[2] Shipboard Scientific Party, Sites 889 and 890, Proc. ODP, Init. Rep. 146, part 1, 147–240, 1994.
[3] Shipboard Scientific Party, Site 888, Proc. ODP, Init. Rep. 146, part 1, 55–126, 1994.
[4] Shipboard Scientific Party, Site 891, Proc. ODP, Init. Rep. 146, part 1, 241–300, 1994.
[5] Shipboard Scientific Party, Site 892, Proc. ODP, Init. Rep., 146, part 1, 301–380, 1994.
[6] R.J. Musgrave, H. Collombat and A.N. Didenko, Magnetic sulfide diagenesis, thermal overprinting, and paleomagnetism of accretionary wedge and convergent margin sediments from the Chile triple junction region, Proc. ODP, Sci. Results, 141, in press.
[7] R. Karlin, Magnetic mineral diagenesis in suboxic sediments at Bettis site W–N, NE Pacific Ocean, J. Geophys. Res. 95, 4405–4419, 1990.
[8] B.W. Leslie, S.P. Lund and D.E. Hammond, Rock magnetic evidence for the dissolution and authigenic growth of magnetic minerals within anoxic marine sediments of the California continental borderland, J. Geophys. Res. 95, 4437–4452, 1990.
[9] D.E. Canfield and R.A. Berner, Dissolution and pyritization of magnetite in anoxic marine sediments, Geochim. Cosmochim. Acta 51, 645–659, 1987.
[10] A.P. Roberts and G.M. Turner, Diagenetic formation of ferrimagnetic iron sulphide minerals in rapidly deposited marine sediments, South Island, New Zealand, Earth Planet. Sci. Lett. 115, 257–273, 1993.

[11] R.L. Reynolds, N.S. Fishman, R.B. Wanty and M.B. Goldhaber, Iron sulfide minerals at Cement Oil Field, Oklahoma: Implications for magnetic detection of oil fields, Geol. Soc. Am. Bull. 102, 368–380, 1990.
[12] R. Lu and S.K. Banerjee, Magnetite dissolution in deep sediments and its hydrologic implication: a detailed study of sediments from Site 808, Leg 131, J. Geophys. Res. 99, 9051–9060, 1994.
[13] E.D. Sloan, Clathrate Hydrates of Natural Gases, 641 pp., Marcel Dekker, New York, 1990.
[14] K.A. Kvenvolden, Gas hydrate — geological perspective and global change, Rev. Geophys. 31, 173–187, 1993.
[15] R.D. Hyndman and E.E. Davis, A mechanism for the formation of methane hydrate and seafloor bottom-simulating reflectors by vertical fluid expulsion, J. Geophys. Res. 97, 7025–7041, 1992.
[16] R. Matsumoto, Isotopically heavy oxygen-containing siderite derived from the decomposition of methane hydrate, Geology 17, 707–710, 1989.
[17] G.D. Ginsburg, V.A. Soloviev, R.E. Cranston, T.D. Lorenson and K.A. Kvenvolden, Gas hydrates from the continental slope, offshore Sakhalin Island, Okhotsk Sea, Geo-Mar. Lett. 13, 41–48, 1993.
[18] W. Lowrie, Identification of ferromagnetic minerals in a rock by coercivity and unblocking temperature properties, Geophys. Res. Lett. 17, 159–162, 1990.
[19] K. Kobayashi and M. Nomura, Iron sulfides in the sediment cores from the Sea of Japan and their geophysical implications, Earth Planet. Sci. Lett. 16, 200–208, 1972.
[20] R. Day, M.D. Fuller and V.A. Schmidt, Hysteresis properties of titanomagnetites: grain size and composition dependence, Phys. Earth Planet. Inter. 13, 260–272, 1977.
[21] M.J. Dekkers, Some rock-magnetic parameters of fine-grained hematite, goethite, and pyrrhotite, Ph.D. Thesis, Univ. Utrecht, 231 pp., 1988.
[22] A.P. Roberts, Magnetic properties of sedimentary greigite (Fe_3S_4), Earth Planet. Sci. Lett. 134, 227–236, 1995.
[23] R.L. Reynolds, M.L. Tuttle, C.A. Rice, N.S. Fishman, J.A. Karachewski and D.M. Sherman, Magnetization and geochemistry of greigite-bearing Cretaceous strata, North Slope Basin, Alaska, Am. J. Sci. 294, 485–528, 1994.
[24] I.F. Snowball and R. Thompson, The occurrence of greigite in sediments from Loch Lomond, J. Quat. Sci. 3, 121–125, 1988.
[25] I.F. Snowball and R. Thompson, A stable chemical remanence in Holocene sediments, J. Geophys. Res. 95, 4471–4479, 1990.
[26] I.F. Snowball, Magnetic hysteresis properties of greigite (Fe_3S_4) and a new occurrence in Holocene sediments from Swedish Lappland, Phys. Earth Planet. Inter. 68, 32–40, 1991.
[27] V. Hoffmann, Greigite (Fe_3S_4): Magnetic proerties and first domain observations, Phys. Earth Planet. Inter. 70, 288–301, 1992.
[28] R.H.W. Bradshaw and R. Thompson, The use of magnetic measurements to investigate the mineralogy of some Icelandic lake sediments and to study catchment processes, Boreas 14, 203–215, 1985.
[29] R. Thompson and F. Oldfield, Environmental Magnetism, 227 pp., Allen and Unwin, London, 1986.
[30] M. Kastner, K.A. Brown, J.-P. Foucher, et al., Gas hydrates and bottom simulating reflectors in the Cascadia Margin, EOS Trans. Am. Geophys. Union 74, 369, 1993.